ADVANCES IN ATMOSPHERIC SCIENCES, VOL. 20, NO. 5, 2003, PP. 815–824

Analysis of Simulated Heavy Rain over the Yangtze River Valley During 11–30 June 1998 Using RIEMS

XIONG Zhe* (熊 喆), WANG Shuyu (王淑瑜), ZENG Zhaomei (曾昭美), and FU Congbin (符淙斌)

Key Laboratory of Climate-Environment for East Asia, IAP., CAS, Beijing 100029

(Received 18 September 2002; revised 12 June 2003)

ABSTRACT

RIEMS' ability to simulate extreme monsoon rainfall is examined using the 18-month (April 1997 September 1998) integrated results. Model-simulated heavy precipitation over the Yangtze River valley during 11–30 June 1998 is compared with the observation, and the relationships between this heavy rainfall process and the large-scale circulations, such as the westerly jet, low-level jet, and water vapor transport, are analyzed to further understand the mechanisms for simulating heavy monsoon rainfall. The analysis results show that (1) RIEMS can reproduce the pattern of heavy precipitation over the Yangtze River valley during 11–30 June 1998，but it is shifted northwestwards. (2) The simulated West Pacific Subtropical High (WPSH) that controls the East Asia Monsoon evolution is stronger than the observation and is extended westwards, which possibly leads to the north westward shift of the heavy rain belt. (3) The Westerly jet at 200 hPa and the Low-level jet at 850 hPa, both of which are related to the heavy monsoon rainfall, are reasonably reproduced by RIEMS during 11–30 June 1998, although the intensities of the simulated Westerly/Low-level jets are strong and the location of the Westerly jet leans to the southeast, which may be the causes of RIEMS producing too much heavy rainfall in the north of the Yangtze River valley.

Key words: RIEMS, heavy rain, low-level jet, westerly jet

1. Introduction

Numerous significant finding have been achieved from the studies of large-scale climate variation by atmospheric general models (Gates, 1992), but these models do not work well in the research of modeling and prediction of regional climate variation (Groth and Mac Cracken, 1991). In recent years, regional climate models have been widely used for high resolution simulation and study of regional climate anomalies. In particular, the Regional Climate Model (RegCM) developed at the National Center for Atmospheric Research (NCAR) has been widely used by the scientific community for simulating regional climate over a range of areas, such as the United States, Sahel, and Europe-East Asia-Pacific. In particular, Gong et al. (1996), Liu et al. (1996), Luo and Zhao (1997), Fu et al. (1998), Wei et al. (1998), and Wei and Wang (1998) used NCAR RegCM and other regional climate models to evaluate the models' ability in simulating the summer climate of East Asia. At present, the study of high resolution RCM simulation has been undertaken mainly in the latest few years in China. In particular, Scientists from START Regional Center for Temperate East Asia(START TEA RRC)

developed the Regional Integrated Environment Model System (RIEMS, Fu et al., 2000) for Asia. In this paper, we use RIEMS to simulate severe flooding in the summer of 1998.

In the summer of 1998, an exceptionally serious flood occurred along the whole Yangtze River, the Nenjiang River, and the Songhua River valleys. The catastrophic flood was mainly caused by three heavy rainfall processes, which occurred respectively on 11–29 June, 21–31 July, and 1–10 August, 1998 (National Climte Center, 1998). In these three heavy rainfall events, the total amount of heavy rainfall during the period of 12–27 June, 1998 increased by 50%–300% in comparison with total precipitation in the same period of a normal year.

According to the study of Ding (1991), more than 75% of heavy rains with a daily rainfall excess of 100 mm are accompanied by the Low-level jet located in South China, North China, and Kyushu, Kobe of Japan, and the main rainfall center often occurs at 0–

*E-mail: xzh@tea.ac.cn

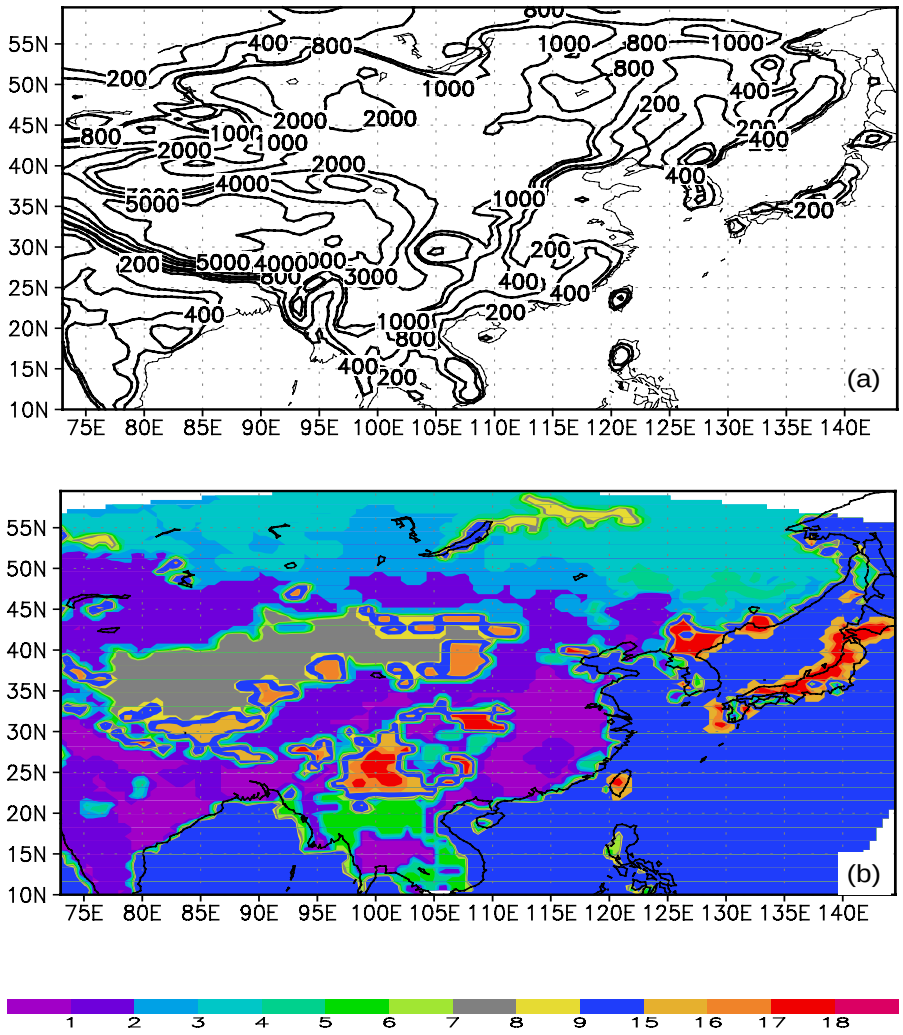

Fig. 1. (a) The topography within the domain (units: m); (b) Model land-use distribution. 1 crop, 2 short grass, 3 evergreen needle, 4 deciduous needle, 5 deciduous broadleaf tree, 6 evergreen broadleaf tree, 7 tall grass, 8 desert, 9 tundra, 15 sea, 16 evergreen shrub, 17 deciduous shrub, 18 mixed tree.

200 km on the left of the Low-level jet axis (Ding, 1991; Palman and Newton, 1969), as well as 300 km away from the right side of the Westerly jet axis. Therefore, heavy rain often appears in the region where the Westerly jet and Low-level jet intersect, where thermal and convective instability often occur, so heavy precipitation often occurs on the left of the Low-level jet axis and on the right side of the Westerly jet axis.

In this paper, the rainfall in the period of 11-30 June, 1998 is selected to study RIEMS' capability to reproduce heavy rain, the Westerly jet and Low-level jet, and the water vapor transport in the East Asia region. The relationships between them are also analyzed and the mechanism that controls the model's simulation of heavy monsoon rainfall is investigated.

2. Model introduction

RIEMS designed by START TEA RRC is used for the simulation. The dynamic component of this model is the same as that of the Penn State/NCAR Mesoscale Model Version 5 (MM5). It is a primitive equation, grid point limited area model with hydrostatic compressible balance written in a terrain-following coordinate system. RIEMS consists of the land surface physics scheme BATS (Dickinson et al., 1986), which has been widely used in climate models, a Holtslag explicit planetary boundary layer formulation (Holtslag et al., 1990), a Kuo-Anthes culumus parameterization, and a modified radiation package (CCM3). Initial and lateral boundary conditions for wind, temperature,

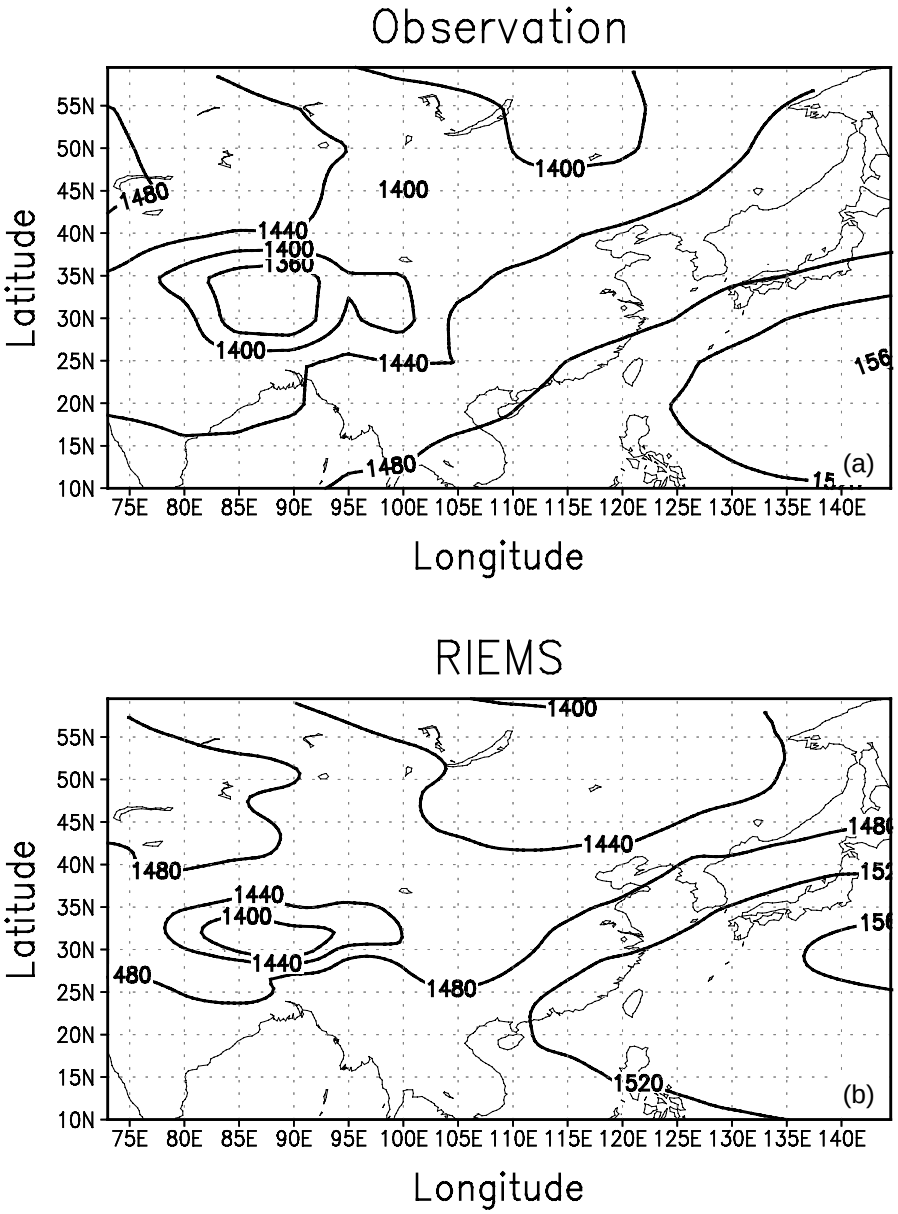

Fig. 2. Mean geopotential height fields at 850 hPa (units: gpm) during 11–30 June, 1998. (a) Observation; (b) RIEMS.

water vapor, and surface pressure are interpolated from NCEP reanalysis data, and the lateral boundary conditions are provided via a linear relaxation scheme and are available at 6-h intervals.

The simulated domain encompasses China, Japan, Korea, India, Mongolia, and Far East Russia (see Fig. 1), with its center located at (35°N, 105°E). The horizontal mesh consists of 151 and 111 grid points in the longitudinal and latitudinal directions respectively with horizontal resolution of 60 km. The simulated period starts from March 1997 and runs to September 1998, which includes a full annual cycle and a hot drought in the summer of 1997 and a severe flood in the summer of 1998. Figure 1 presents the topography and land cover type within the domain.

3. Data for validation and method

The dataset for validation contains both station data and grid data. The daily precipitation data are collected from 591 observation stations in Mongolia, the Korean Peninsula, Japan, China, India and Russia. Over the region where sparse station data are available, both $5° \times 5°$ degree pentad U, V wind compo-

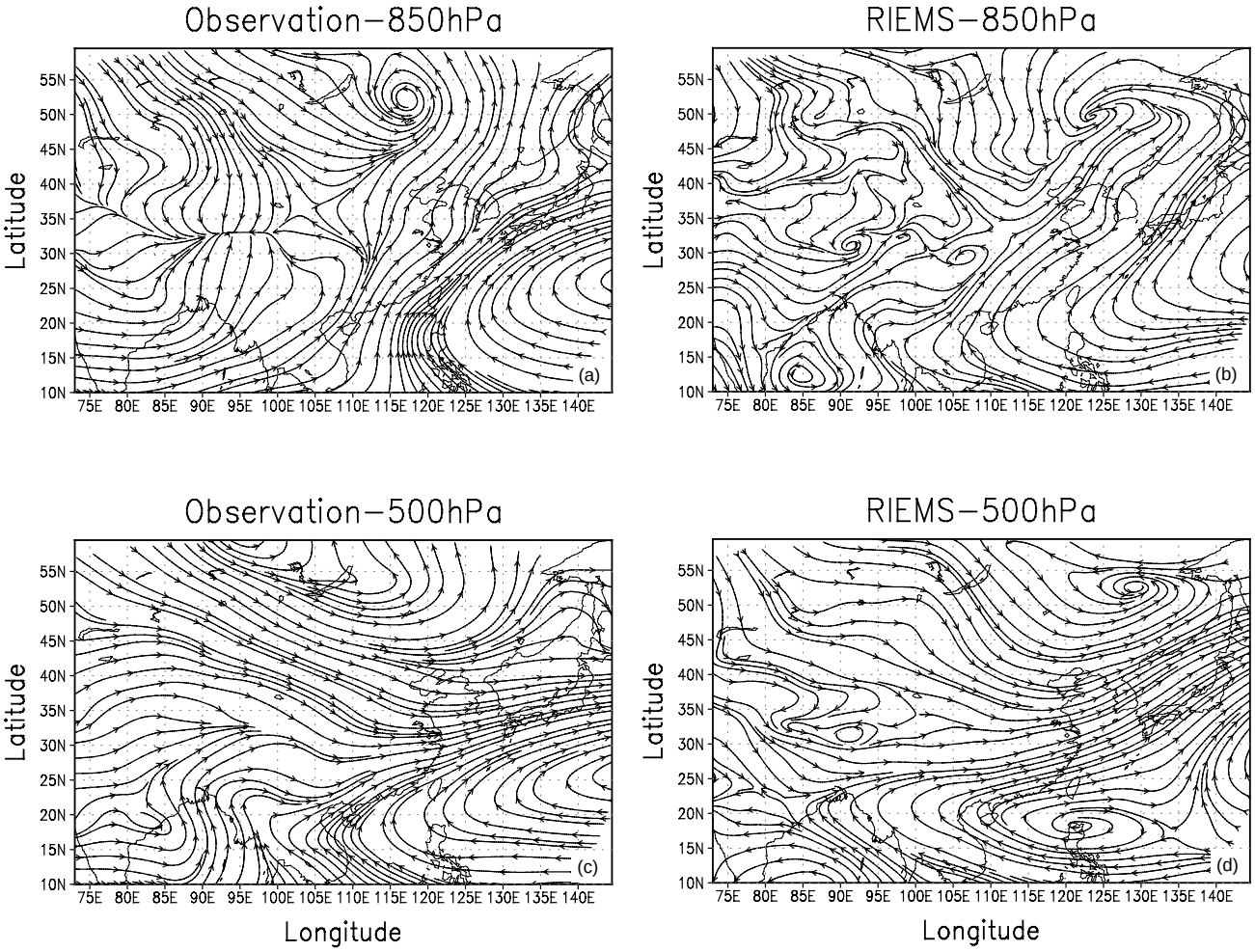

Fig. 3. Mean streamline fields during the period of 11–30 June 1998. (a) Observation at 850 hPa; (b) RIEMS at 850 hPa; (c) Observation at 500 hPa; (d) RIEMS at 500 hPa.

nents (unit: m s^{-1}), geopotential height (unit: gpm), upper level temperature (°C) from JMA* and the relative humidity (RH, in %) from the NCEP reanalysis dataset used to calculate the specific humidity (q) are utilized in validation.

The Westerly jet (or referred to as the Upper-level jet) is defined as existing when the wind speed is greater than 60 m s^{-1}, and the critical value of 14 m s^{-1} is used for the low-level jet(Ding, 1991; Zhai, 1999).

4. Results

4.1 *Geopotential height fields and streamline fields*

Figure 2a depicts the observed mean geopotential height fields at 850 hPa during 11–30 June 1998. There are two planetary scale circulations that dominate the East Asia summer monsoon in the geopotential height fields: (1) the WPSH is illustrated by the 1520-gpm line reaching the southeast of Japan; and (2) the Asian low over the continent whose trough covers 2/3 of themodel domain.

The simulated geopotential height pattern agrees with the observations, but the strength of the simulated WSPH is stronger, with the simulated 1520-gpm line extending to the continent.

Figure 3 illustrates the mean streamline fields at 850 hPa and 500 hPa during the same period. Two planetary scale circulations occur in the observation: One is the WSPH and the other is the mid-latitude cyclone in the northern part of the domain, which can be identified in the observation. RIEMS can reproduce

* Provided by the Computing and Information Science Center of IAP.,CAS.

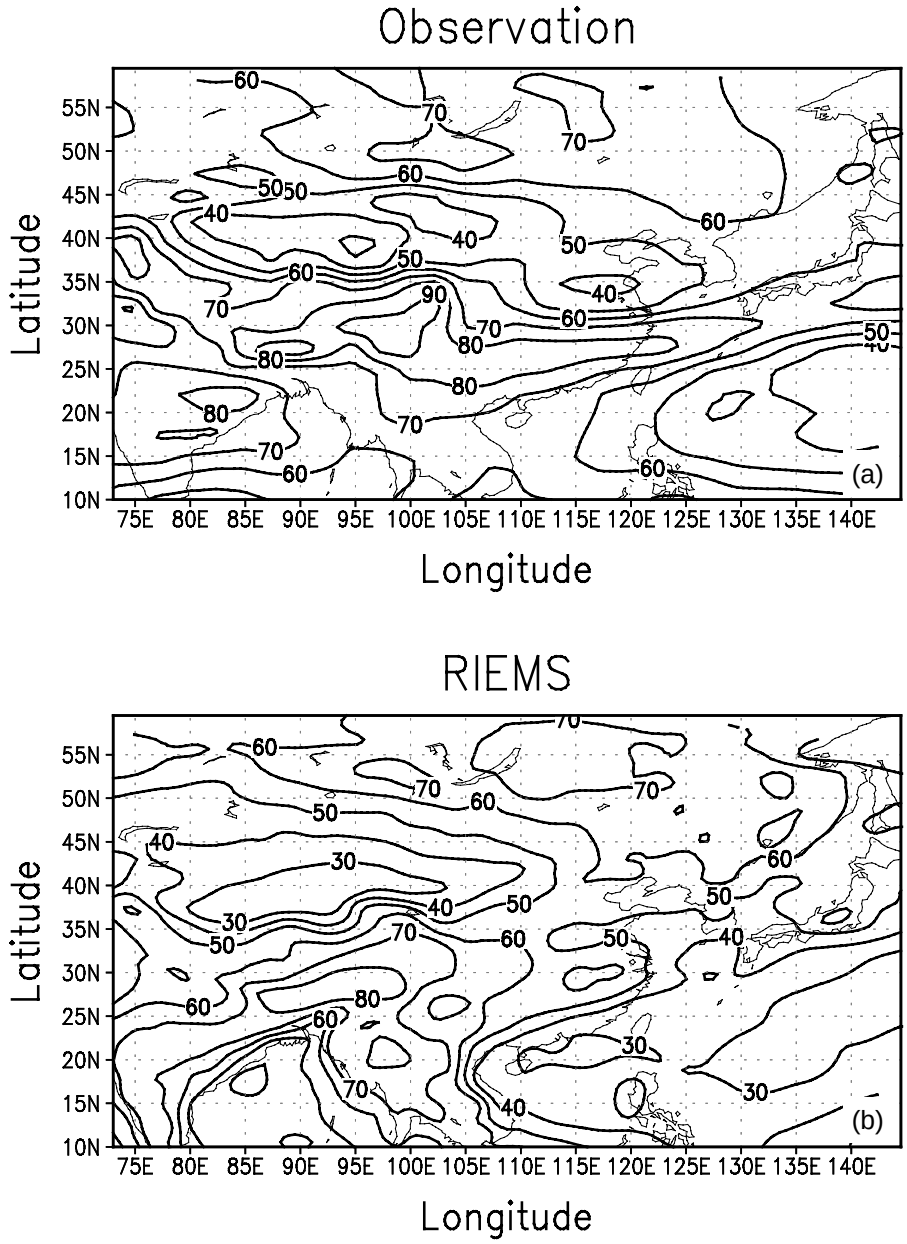

Fig. 4. Mean relative humidity at 700 hPa in the period of 11–30 June 1998. (a) Observation; (b) RIEMS.

the observed large-scale circulation, though the WPSH both at 850 hPa and 500 hPa stretches out northwestwardly. The simulated WPSH at 500 hPa splits into two centers with one of them over the Philippines, leading to the northwest shift of the southwesterly flow in the rear of the WPSH. The induced northwest shifts of the Low-level jet by the northwest shift of this southwesterly flow might cause the simulated heavy rainfall center to move into the northwest region of the Yangtze River valley.

4.2 *Relative humidity and water vapor transport*

Figure 4 shows the observed and simulated mean relative humidity at 700 hPa during 11–30 June 1998, indicating that the distributions of dry and wet areas at 700 hPa are captured reasonably well by RIEMS. However, the model tends to be drier compared to the observation. For two low RH centers over the West Pacific Ocean and Northwest China, the model simulations are drier with more areas having relative hu-

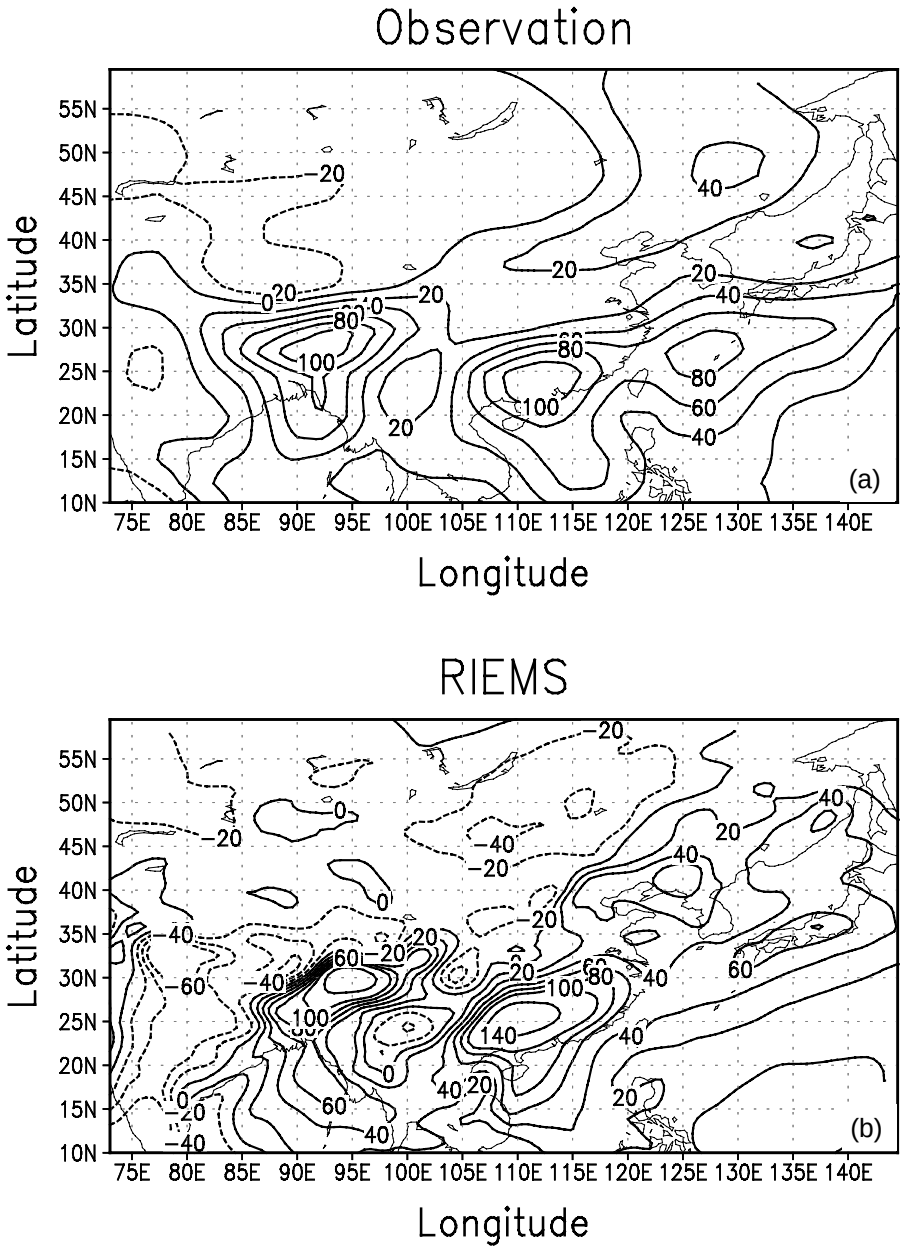

Fig. 5. Mean water vapor transport (q×v) at 850 hPa in the period of 11–30 June 1998. (a) Observation; (b) RIEMS.

midity less than 40% (dark shadow area in Fig. 4a). Over the high RH area of the Tibetan Plateau and south of the Yangtze River valley, the simulated RH is smaller, and areas with relative humidity greater than 80% (gray shadow in Fig. 4b) are reduced. The observed higher relative humidity belt is in an east-west orientation and lies over the south of the Yangtze River valley, but the simulated high value belt exhibits a northeast-southwest orientation and the range of the simulated high value belt is smaller than that of the observation . This might imply that the lack of water vapor in the atmosphere results in the absence of the simulated heavy rain belt over the south of the Yangtze River valley and South China (see Fig. 7).

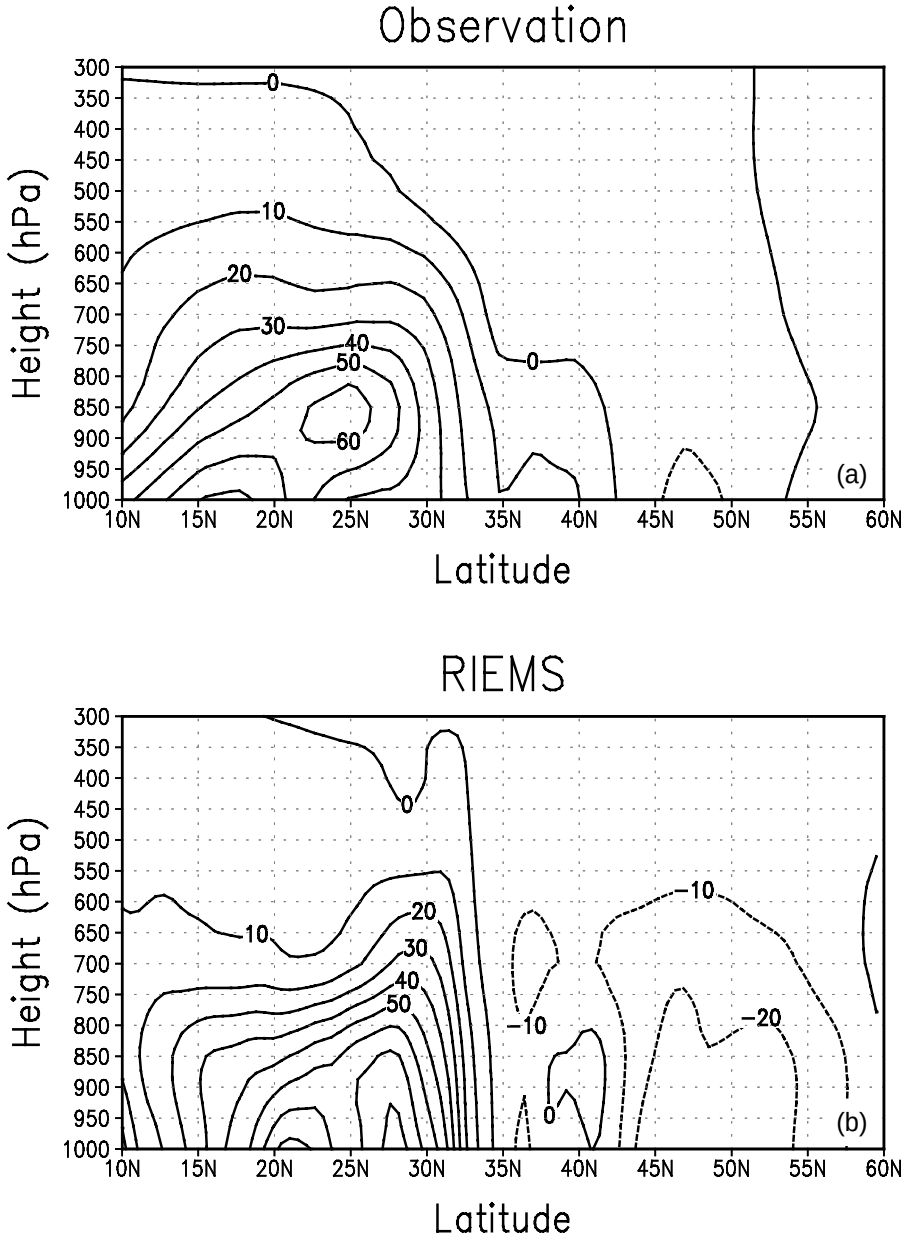

Fig. 6. 100°–120°E mean vertical cross-section of the water vapor transport during 11–30 June 1998. (a) Observation; (b) RIEMS.

The observed and simulated water vapor transports, which are expressed by the specific humidity q multiplied by the V component ($\mathrm{m\,s^{-1}}$) at 850 hPa, are shown in Fig. 5. RIEMS reproduces the three transport centers over the West Pacific, South China, and the Tibetan Plateau properly, as well as the relatively drier water vapor transport belt running from Southwest China to Northeast China, which clearly demonstrates the two separate water vapor sources from the Bay of Bengal and the West Pacific Ocean. The simulated transport centers over the Tibetan Plateau and South China are stronger than the observation, but the other one over Southwest Japan is weaker and its position is shifted towards the northeast compared with the observation. This result is in agreement with the study of Xu et al. (2003), which pointed out the main body of the water cycle that formed the torrential rain in the Yangtze River valley was made up of water va-

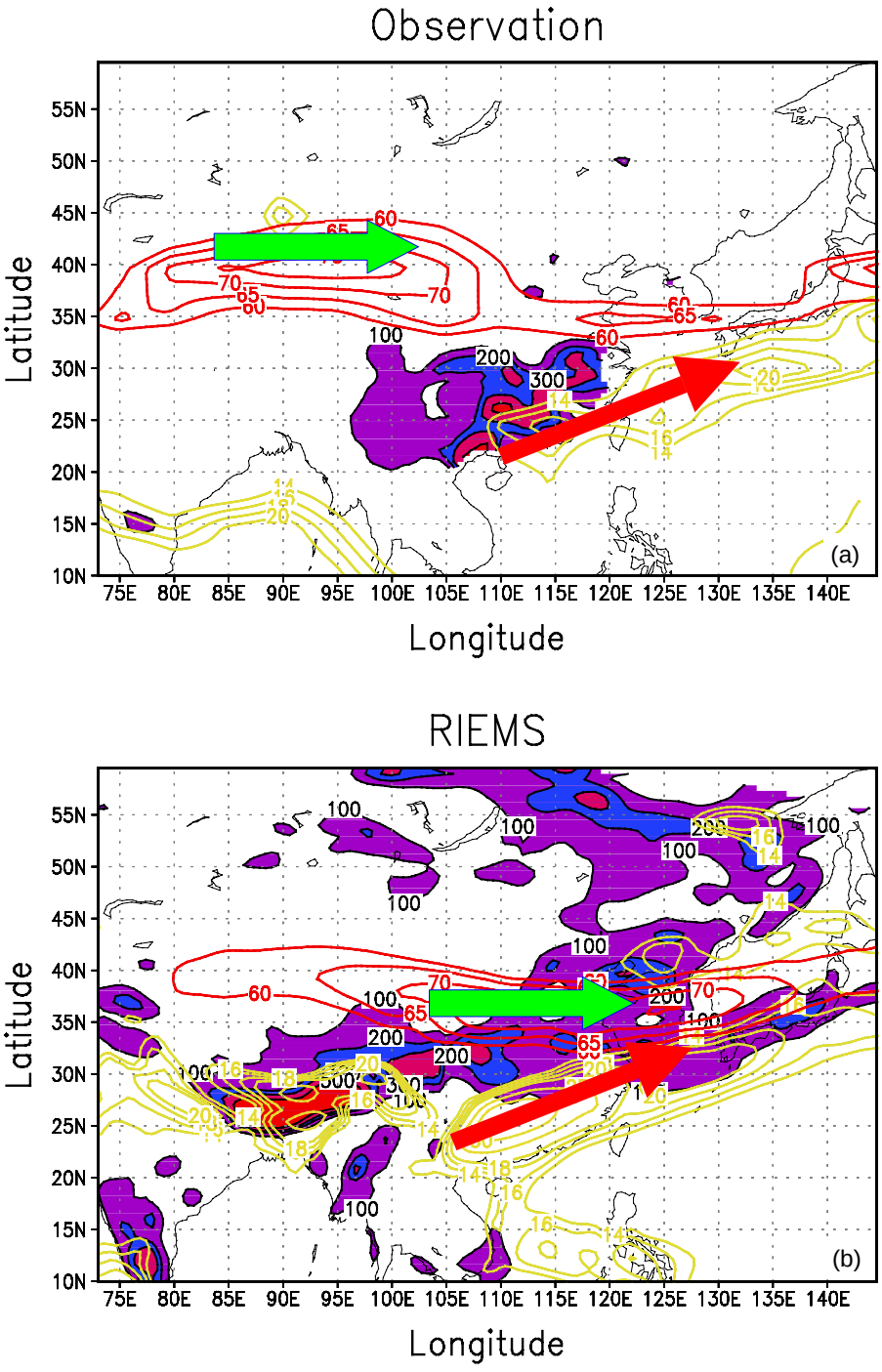

Fig. 7. The distribution of total precipitation over 100 mm and the location of the Westerly jet at 200 hPa and Low-Level jet at 850 hPa during the period of 11–30 June 1998. (a) Observation; (b) RIEMS.

por transport at the western and southern boundaries of the China region during the period of 11–20 June 1998, and the southern boundary of China played an important role in the torrential rain in the Yangtze River valley.

Figure 6 shows the 100°–120°E mean vertical cross-section of the water vapor transport during the period of 11–30 June 1998. From the comparison between the observation and simulation, it can be seen that RIEMS reproduces the vertical distribution of the wa-

ter vapor transport well. However, the locations of the simulated maximum water vapor transport center are shifted northward by about 5 degrees in Fig. 6b and the magnitudes are stronger than the observation; so the simulated heavy rain belt by RIEMS moves into the northwest of the Yangtze River valley with much more precipitation.

4.3 *The precipitation and Westerly and Low-level jets*

Figure 7a shows the observed total precipitation, the Westerly jet at 200 hPa, and Low-level jet at 850 hPa during the period of 11-30 June 1998. For the Low-level jet, the observed largest wind speed center (shown in Fig. 7a) is located on the West Pacific Ocean to the southeast of the Japan Islands, with the maximum wind speed of $20\,\mathrm{m\,s^{-1}}$, and the simulated largest wind speed center is in Southeast China with the maximum wind speed exceeding $30\,\mathrm{m\,s^{-1}}$ (see Fig. 7b). For the Westerly jet, the observed center is located in the east of Xinjiang, however, the simulated Westerly jet center is shifted southeastwards.

The model can reproduce the location of the observed heavy rainfall center to the left of the Low-level jet axis, but on the right side of the Westerly jet axis, however, the heavy rainfall belt with total precipitation over 300 mm simulated by RIEMS (see the yellow shadow area in Fig. 7b) is placed far too westwards near the Tibetan Plateau and the northwest part of the upper reaches of the Yangtze River in comparison with the observed position of the heavy rain belt, which is located in the middle and lower reaches of the Yangtze River valley and South China.

In general, the occurrence of this heavy rainfall is accompanied by the Westerly jet and Low-level jet. Partly because of the southwest shift of the simulated Low-level jet and southeast shift of the simulated Westerly jet, RIEMS' main rain belt drifts to the northwest of the Yangtze River valley.

5. Summary and discussion

Base on the above analyses, we find the following.

(1) RIEMS can reproduce the pattern of heavy precipitation over the Yangtze River valley during 11–30 June 1998，but its position is shifted northwestward.

(2) RIEMS can reproduce well the locations of the Westerly jet at 200 hPa and the Low-level jet at 850 hPa in East Asia. But both the Westerly jet and the Low-level jet are simulated far stronger than the observations. The center positions of the maximum wind speed for the Westerly and Low-level jets are shifted southeastwards and southwestwards, respectively, in comparison with the observations, which may explain the RIEMS model producing too much rainfall to the north part of the Yangtze River valley.

(3) The simulated West Pacific Subtropical High is stronger and its location is extended too far westwards, which possibly leads to the northwestwards shift of the heavy rain belt.

(4) RIEMS can capture the main characteristics of the water vapor transport and the distribution of the relative humidity during the heavy rain period, but the allocations of the heavy rainfall belt and the strongest water vapor center do not match well.

In general, the shift of the main rain belt by RIEMS is caused not only by the northwest ward shift of the Low-level jet or induced by the strong and northwest-extending West Pacific Subtropical High, but also by the lack of water vapor in South China and the middle-lower reaches of the Yangtze River valley, and by the northward shift of the maximum water vapor transport center. The differences of the West Pacific Subtropical High, Westerly jet, Low-level jet, and precipitation between the observations and the simulations are related to the model's internal physical scheme including the convective parameterization, the horizontal advection scheme, and the model's handling of complex regions such as the Tibetan Plateau. Further simulation is necessary to test the modifications to the present schemes, as well as the use of alternate convection schemes, which is expected to improve the model's shortcomings over complex regions.

Acknowledgments. This project was supported by the National Key Program for Developing Basic Sciences (G1999043403) and the Program for Knowledge Innovation Project, Chinese Academy of Sciences (KZCX3-SW-218).

REFERENCES

Dickinson, R. E., P. J. Kennedy, A. Henderson-Sellers, and M. Wilson, 1986: Biosphere-Atmosphere Transfer Scheme (BATS) for the NCAR Community Climate Model. Tech. Note, NCAR/TN-275+STR, National Center for Atmospheric Research, Boulder, CO, 69pp.

Ding Yihui, 1991: *Advanced Synoptic Meteorology*, China Meteorological Press, 792pp.

Fu Congbin, Wei Helin, Chen Ming, Su Bing Kai, Zhao Ming, and Zheng Weizhong,1998: Simulation of the evolution of summer monsoon rainbelts over eastern China from regional climate model. *Chinese Jounal of Atmospheric Sciences*, **22**(4), 522–534.

Fu Congbin, Wei Helin, and Qian Yun., 2000: Documentation on Regional Integrated Environmental Model System (RIEMS, Version I). TEACOM Science Report, No, 1, START Regional Committee for Temperate East Asia, Beijing, China, 36pp.

Gates, W. L., 1992: The atmospheric model intercomparison Project. *Bull. Amer. Meteor. Soc.,* **73**, 1962–1970.

Gong Wei, Li Weiliang, and Zhou Xiuji, 1996: Modeling summer precipitation in China by a modified NCAR RegCM. *Studies on Short-term Climate Variations and Their Formation in China*, Cao Hongxing, Li Yuehong, Wei Fengying, Eds., China Meteorological Press, Beijing, 110–116. (in Chinese)

Groth, S. L., and M. C. MacCracken, 1991: The use of general circulation models to predict regional climate change. *J. Climate*, **4**, 286–303.

Holtslag, A. A. M., E. I. F. de Bruijin, and H. L. Pan, 1990: A high resolution air mass transformation model for short range weather forecasting. *Mon. Wea. Rev.*, **118**, 1561–1575.

Liu Yongqiang, R.Avissar, and F. Giorgi, 1996: A simulation with the regional climate model RegCM2 of extremely anomalous precipitation during the 1991 East-Asian flood: An evaluation study. *J. Geophys. Res.*, **101**, 26 199–26 215.

Luo Yong, and Zhao Zongci, 1997: Numerical simulation of East Asia regional climate with NCAR RegCM2. *Quarterly Journal of Applied Meteorology*, 8(Suppl.), 124–133. (in Chinese)

National Climate Center, 1998: *China Climate Impact Assessment,* China Meteorological Press, 34pp.

Palmen, E., and C. W. Newton, 1969: *Atmospheric Circulation Systems*. International Geophysics Series, Vol. 13, Academic Press, New York and London, **13**, 471–560.

Wei Helin, Fu Congbin, and W. C. Wang, 1998: The effect of lateral boundary treatment of regional climate model on the East Asian summer monsoon rainfall simulation. *Chinese Journal of Atmospheric Sciences*, **22**(3), 231–243.

Wei Helin, and W. C. Wang, 1998: A regional climate model simulation of summer monsoon over East Asia: A case study of 1991 flood in Yangtze-Huaihe valley. *Advances in Atmospheric Sciences*, **15**(4), 489–509.

Xu Xiangde, Miao Qiuju, Wang Jizhi, and Zhang Xuejin, 2003: The water vapor transport model at the regional boundary during the Meiyu Period. *Advances in Atmospheric Sciences*, **20**(3), 333–342.

Zhai Guoqing, Ding Huajun, Sun Shuqing, 1999: Physical Characteristics of Heavy Rainfall Associated with Strong Low-level Jet. *Chienese Journal of Atmospheric Sciences*, **23**(1), 112–118.